Computation of turbulent separated nozzle flows

Q. Xiao and H.M. Tsai

Temasek Laboratories, National University of Singapore, 10 Kent Ridge Crescent, Singapore 119260, Singapore

Abstract. The computationally challenging case of an over-expanded nozzle flow involving shock induced boundary layer separation is examined in this paper. Comparative studies using a base line two-equation $k - \omega$ turbulence model with and without taking into account non-equilibrium effects are made. The additional equation (the lag equation) to model non-equilibrium effect for the eddy viscosity in the separated flow region, significantly improves predictions of shock induced separated flows in exhaust nozzle.

1   Introduction

Flow separations usually occur in convergent-divergent (CD) nozzles, where the nozzle expansion ratio is too large for a given nozzle pressure ratio (NPR). In general supersonic nozzle flow expands to a pressure level that is far lower than the ambient pressure. As a consequence, a shock is formed to adapt to the ambient conditions thus incurring energy losses. For some nozzles the flow separates and thus generate large unpredictable side-loads to the nozzle. Earlier studies such as those by Asbury, et al. [1] and Hunter [2] showed that off-design nozzle thrust efficiency could be improved by controlling the location and extent of that separation.

Computational simulation of separated turbulent flow poses several difficulties. Turbulent separated flows induced non-equilibrium effects that make it harder to deal. The numerical prediction of separated nozzle flows and the internal flow performance has been the subject of previous studies (see Hunter[3], Carlson [4]). Both made used of NASA Langley Reynolds-averaged Navier-Stokes CFD code (PAB3D). Lower order models, such as two-equation turbulence model are incapable of accounting directly for non-equilibrium effects. More complex Reynolds stress models address this problem. In Hunter's study, two-equation $k - \varepsilon$ turbulence closure with non-linear algebraic Reynolds stress models are applied. In general, their computations are in excellent agreement with experimental data but studies show this approach as difficult for practical use. The complexity and the associated numerical stiffness requires very fine grid resolutions make the model computationally expensive. More recently Olsen and Coakley [5] proposed a different approach. The central idea is to take a baseline two-equation model and couple it with a third (lag) equation to model the non-equilibrium effects for the eddy viscosity. Xiao et al.[6] exploited this approach and incorporated the lag model with the baseline $k - \omega$ turbulence model and conducted turbulent simulation for steady and unsteady diffuser flow. Their computational results show significant improvements over results without lag model for separated flow cases.

The aim of the present paper is to explore further the lag models capability for separated nozzle flows. The experimental test by Hunter[3] of a 2-D axi-symmetric convergent-divergent nozzle is used as benchmark. Comparisons of computations with the $k - \omega$ model with and without the lagged equations are presented.

In the following sections, the governing equations and the numerical methods are outlined briefly. This is followed by discussions of the numerical results and conclusions.

2   Computational models

The governing equations for the unsteady compressible turbulent flow with the $k - \omega$ and lag model are expressed as follows:

Mass conservation:

$$\frac{\partial \rho}{\partial t} + \frac{\partial}{\partial x_j}(\rho u_j) = 0 \tag{1}$$

Momentum conservation:

$$\frac{\partial (\rho u_i)}{\partial t} + \frac{\partial}{\partial x_j}(\rho u_i u_j) = -\frac{\partial p}{\partial x_i} + \frac{\partial}{\partial x_j}(\bar{\tau}_{ji}) \tag{2}$$

Mean energy conservation

$$\frac{\partial (\rho E)}{\partial t} + \frac{\partial}{\partial x_j}(\rho u_j H) = \frac{\partial}{\partial x_j}\left[u_i \bar{\tau}_{ji} + (\mu + \sigma^* \mu_T)\frac{\partial k}{\partial x_j} - q_j\right] \tag{3}$$

Turbulent mixing energy:

$$\frac{\partial (\rho k)}{\partial t} + \frac{\partial}{\partial x_j}(\rho u_j k) = \tau_{ij}\frac{\partial u_i}{\partial x_j} - \beta^* \rho \omega k + \frac{\partial}{\partial x_j}[(\mu + \sigma^* \mu_T)\frac{\partial k}{\partial x_j}] \tag{4}$$

Specific dissipation rate:

$$\frac{\partial (\rho \omega)}{\partial t} + \frac{\partial}{\partial x_j}(\rho u_j \omega) = \frac{\varepsilon \omega}{k}\tau_{ij}\frac{\partial u_i}{\partial x_j} - \beta \rho \omega^2 + \frac{\partial}{\partial x_j}[(\mu + \sigma \mu_T)\frac{\partial \omega}{\partial x_j}] \tag{5}$$

Turbulent eddy viscosity:

$$\frac{\partial (\rho \nu_t)}{\partial t} + \frac{\partial}{\partial x_j}(\rho u_j \nu_t) = a(R_t)\omega \rho(\nu_{tE} - \nu_t) \tag{6}$$

The total energy and enthalpy are $E = e + k + u_i u_i/2$ and $H = h + k + u_i u_i/2$, respectively, with $h = e + p/\varrho$ and $e = p/[(\gamma - 1)\rho]$. Other quantities are defined as: $\mu_T = \rho \nu_t$, $\nu_{tE} = \varepsilon^* k/\omega$ and $R_T = \rho k/\mu \omega$

$$S_{ij} = \frac{1}{2}(\frac{\partial u_i}{\partial x_j} + \frac{\partial u_j}{\partial x_i}) \tag{7}$$

$$\tau_{ij} = 2\mu_T(S_{ij} - \frac{1}{3}\frac{\partial u_k}{\partial x_k}\delta_{ij}) - \frac{2}{3}\rho k \delta_{ij} \tag{8}$$

$$\bar{\tau}_{ij} = 2\mu(S_{ij} - \frac{1}{3}\frac{\partial u_k}{\partial x_k}\delta_{ij}) + \tau_{ij} \tag{9}$$

$$q_j = -(\frac{\mu}{Pr_L} + \frac{\mu_T}{Pr_T})\frac{\partial h}{\partial x_j} \tag{10}$$

$$a(R_T) = a_0[\frac{(R_T + R_{T0})}{(R_T + R_{T\infty})})] \tag{11}$$

The closure constants used in the preceding equations are $a_0 = 0.35$, $R_{T0} = 1$, $R_{T\infty} = 0.01$, $\epsilon = \frac{5}{9}$, $\epsilon^* = 1$, $\beta = 0.075$, $\beta^* = 0.09$, $\sigma = 0.5$, and $\sigma^* = 0.5$

Olsen and Coakley [5] pointed out that conventional one and two equation turbulence models generate Reynolds stresses that respond too rapidly to changes in mean flow conditions partially due to the need to accurately reproduce equilibrium flows. As a result, these base line turbulence models give unsatisfactory results for flows with significant separation under adverse pressure gradients or across shock waves. In the above formulations, the standard $k - \omega$ turbulent model are only used to predict the 'equilibrium' eddy viscosity ν_{tE}. The additional equation, Eq. (6), is used to predict the actual eddy viscosity ν_T. This lag equation is essentially a relaxation model

intended to account for memory effects of the turbulence eddy viscosity in adjusting to its local equilibrium value.

The basic numerical method used to solve the above system of equations in this paper follows that described in detail by Liu and Ji [7] and Xiao et al.[6]. The governing equations are discretised in space using finite volume approach. Cell-centred and cell-vertex scheme are used for Navier-Stokes equations and the turbulent equations. The dual time stepping method proposed by Jameson [8] is adopted here for the time discretization in the code but the implicit time accurate part is not relevant since steady state cases are considered in the present study. Local time stepping, residual smoothing and multigrid techniques are also used to accelerate the solution for the Navier-Stokes and turbulence model equations.

3   Test case

The geometry of the 2-D non-axisymmetric convergent-divergent nozzle is shown in Fig. 1a. The experimental tests by Hunter[3] was made for an NPR range from 1.25 to 9.5. As noted by Hunter the flow is only truly 2-D for NPR greater than 2.4. The computational domain (see Fig. 1b) includes the ambient region that extends 30 throats heights downstream, 25 throat heights upstream, and 25 throat heights normal to the jet axis. The grid cells used in the computation is 1216x128. The C-grid topology used therefore involves having some grids being excluded from the computation. The grid was designed for the Reynolds number based on throat height of 3.2 million, with the minimum first grid point near wall of $y^+ < 1$.
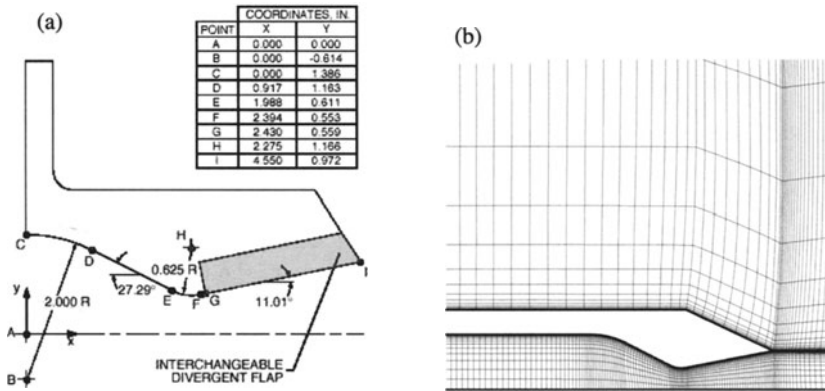

Fig. 1. Geometry of nozzle and grid distribution. (a) Geometry of nozzle (figure from Hunter[3]) (b) Grid distribution 1216x128 mesh (For clarity, grid is drawn by skipping 4 grid lines in each directions)

At the inlet boundary, $p_t = NPR \times p_a$, $T_t = T_a$ where p_t is the total pressure, p_a is the static ambient pressure equal to $14.85(psi)$, T_t is the total temperature set at $530R$. The value of ω is estimated as $\omega = O(10u/h)$, where u is the velocity at the inlet boundary and h is the height of throat. The k is specified with a small value to keep the inlet eddy viscosity at a low level. The eddy viscosity ν_t is set to ν_{tE}. At the outlet boundary, only the pressure is specified as the ambient pressure p_a and all the other variables are extrapolated. Characteristic boundary condition is specified at the far-stream, and symmetric boundary condition is specified at the center-line of the nozzle. At the wall, zero velocity is imposed and the pressure is extrapolated to the wall. Also the k is set to zero and ω must satisfy the asymptotic solution $\omega \rightarrow \frac{6\nu_w}{\beta y^2}$ as the wall is approached. Here the eddy viscosity ν_t is set to its equilibrium value ν_{tE}.

4   Results and discussions

Fig. 2a and 2b show the computed as well as the experimental data of the wall pressure distribution for NPR<5.4 and NPR>5.4. The computational results do not agree well with experiments for NPR<2.4. This is similar to the results of Hunter[3], and due to the non two-dimensionality of the flow under the condition of NPR<2.4. It is evident that with increasing NPR, the computational results agree well with the experiments. For NPR>5.4, all the data coincide onto one curve, which is in good agreement with experimental data and results of Hunter[3]. Similar results for two higher NPR values (NPR=7.0, 8.74) are obtained, but not included in the figure. They show for NPR>5.4, the flow in the nozzle is essentially shock free, and the lag model plays no significant part.
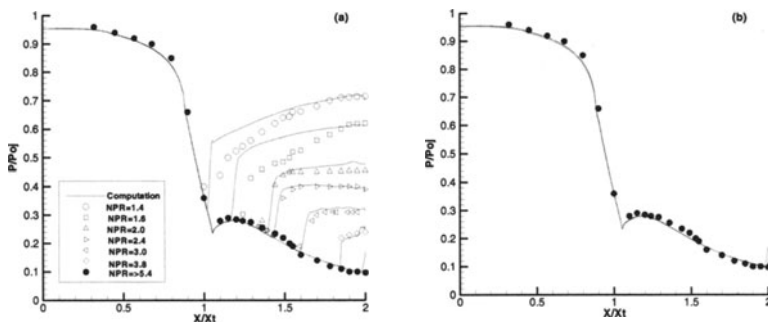

Fig. 2. Comparison of calculated pressure distribution (with Lag model) with experimental data (from Hunter[3]). Symbols: experiment; Lines: calculation results. (a) NPR<5.4, (b) NPR>5.4

The comparisons of computational results with and without the lag model are shown in Figs.3 and 4. Figs.3a and 3b show the pressure distributions on the top wall for NPR=2.4 and 3.0 respectively. As shown, the calculations with the lag model accurately predict the pressure distribution and shock location similar to the experimental data. However, the prediction without the lag model displays a further downstream shock location compared to the experiment.

The Mach contour comparisons with and without lag model are shown in Figs.4 and 5 for NPR=2.4 and 5.4 respectively. It can be seen that, the lambda shock location predicted by lag model is obviously more upstream than that predicted without the lag model for NPR=2.4 and more consistent with the experiment. For NPR>5.4 where there are no separated flow regions, there is no noticeable differences for computations with the lag or without the lag model.

5   Conclusions

A computational study of turbulent separated nozzle flow has been conducted using a multigrid finite-volume method. The base line $k - \omega$ model is used with and without including the lagged model. Computational results are compared to experimental data reported by Hunter[3]. The impact of the lag model on the predicted flow is very significant offering accurate computations of shock induced separated flows within the nozzle. The computations are in good agreement with the experimental data for NPR>2.4. For higher NPR (NPR>5.4), where separated flow is absent, the effect of the lag model is negligible.
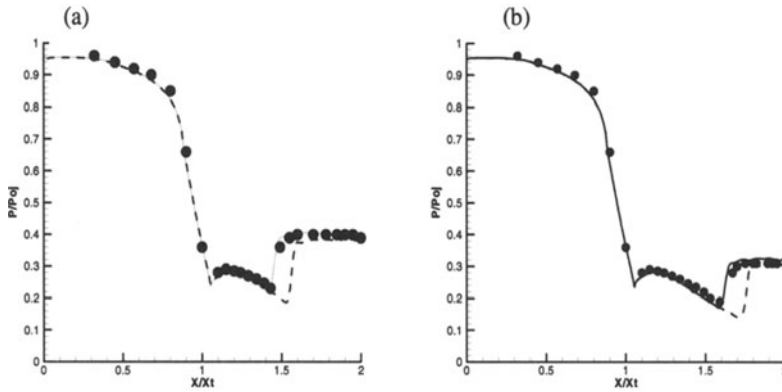
Fig. 3. Top wall pressure distribution: (a) NPR=2.4; (b) NPR=3.0. Circle: experiment; Dashed line: without lag model; Solid line: with lag model
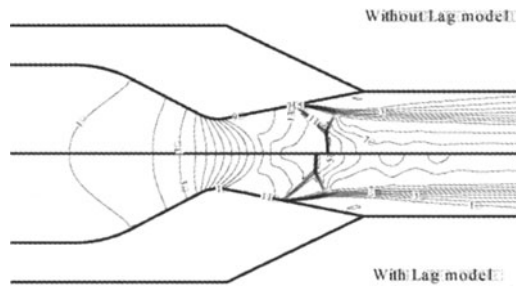

Fig. 4. Mach contour with lag and without lag model (NPR=2.4). Mach contour range is from 0.24-1.71, dMa=0.24.
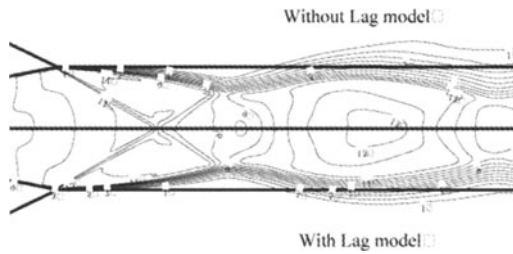

Fig. 5. Mach contour with lag and without lag model (NPR=5.4). Mach contour range is from 0.24-1.71, dMa=0.24.

References

1. S.C. Asbury, C.L. Gunther, C.A. Hunter: A passive cavity concept for improving the off-design performance of fixed-geometry exhaust nozzles. AIAA 96-2541 (1996)
2. C.A. Hunter: An Experimental Analysis of Passive Shock-boundary Layer Interaction Control for Improving the Off-design Performance of Jet Exhaust Nozzles. M.S. Thesis, The George Washington University JIAFS. (1993)
3. C.A. Hunter: Experimental, theoretical, and computational investigation of separated nozzle flows. AIAA 98-3107 (1998)
4. J.R. Carlson: A nozzle internal performance prediction method. NASA Technical Paper 3221 (1992)
5. M.E. Olsen, T.J. Coakley: The lag model, a turbulence model for non equilibrium flows. AIAA 2001-2564 (2001)
6. Q. Xiao, H.M. Tsai, F. Liu: Computation of transonic diffuser flows by a lagged $k - \omega$ turbulence model. Journal of Propulsion and Power **19(3)**, (2003)
7. F. Liu, S.H. Ji: Unsteady flow calculations with a multigrid Navier-Stokes method. AIAA Journal **34(10)**, 2047 (1996)
8. A. Jameson: Time dependent calculations using multigrid, with applications to unsteady flows past airfoils and wings. AIAA Paper 91-1596 (1991)